Channel Interference in Optical Collisions of Cold Atom Beams

Vladimir A. Yurovsky and Abraham Ben-Reuven*

School of Chemistry, Tel Aviv University, 69978 Tel Aviv, Israel

Received: April 24, 1998

Experiments were conducted recently (by Weiner and co-workers) on the optical shielding (suppression) of atomic collisions in cold-atom beams, and its variation with the angle between the polarization direction of the shielding light and the direction of approach of the beam. This case is shown here to be a typical example of an optical collision in which quantum interference may persevere between two incident collision partial waves leading to the same output state. This effect depends on the relative collisional phase shift of the two interfering channels, as well as on the angle of approach, and will vanish when averaging over the latter (as with collisions in the bulk). The extent of variation of this interference effect with the relative phase shift is quite broad, and may lead, under favorable conditions, to almost complete shielding at a finite value of the shielding-laser power. The latter observation leaves open the possibility of exerting coherent control over the interference effect in order to optimize the shielding.

1. Introduction

The need to shield cold atoms (in the mK regime and below) from loss-inducing collisions has drawn recently some attention (see refs 1−7 and the reviews refs 8 and 9 with references therein). Optical shielding[5−7] was originally supposed to produce better suppression of collisions by increasing the intensity of the shielding-inducing laser beam. This expectation was based on the mechanism of a single Landau−Zener (LZ) transition. The laser radiation, tuned to the blue of the atomic resonance transition, was supposed to couple the ground electronic state of the collision pair to an excited (repulsive) state. By the ensuing phenomenon of avoided crossing, the probability of the atoms approaching each other (to within range of loss-inducing processes) was supposed to decrease exponentially as a function of the laser power. Experiments show that, instead of decreasing exponentially, the penetration probability rather tends to level off, producing incomplete shielding at the higher power levels[5−7].

A simple model, explaining the main reason for incomplete shielding in cold traps of metastable Xe atoms,[3] has been suggested recently by the authors.[1] This model of multiple curve crossing gives a three-dimensional description of the shielding process. The atoms, on approaching the shielding Condon point at the ground electronic state in a given partial wave, may end up penetrating the inner zone again in the ground electronic state, but in a higher partial wave, even at high laser powers. The process is basically of the kind $g, J \rightarrow e, (J+1) \rightarrow g, (J+2)$, where g and e are respectively the ground and excited electronic states, and J is the angular momentum (including the relative motion of the atoms). The treatment of this model was based on a theory of multiple curve crossing processes,[10] drawn from the similarity to a well-known exactly soluble problem of linear potentials.

The effect discussed above is actually incorporated in more rigorous quantum close-coupling (QCC) calculations, as used in the analysis of optical shielding in cold Na traps.[2] Careful analysis shows, however, that in the case of Na, the incomplete shielding effect can be attributed in part also to certain "counterintuitive" transitions, which are not allowed in semiclassical models of multiple curve crossing, as well as in the linear potential model. These transitions correspond to the scheme $g,J \rightarrow e,J-1 \rightarrow g,J-2$ (see Figure 1). An extension of the model of linear potentials to piecewise linear potentials can also provide counterintuitive transitions comparable to those of the QCC theory.[11]

The experiments of Weiner and co-workers on cold atom beams[12] have diverted the attention to the question of optical shielding in beams vs shielding in traps, with their isotropy of atomic motion. The experiments show that the shielding, using linearly polarized light, produces significant dependence on the polarization direction (relative to the direction of approach of the beam).

This breaking of symmetry in the beam should have yet another consequence. Whereas, in the bulk, the total rate of a collision process (such as the penetration probability) can be written as a sum of independent contributions of incident partial waves, this is no more the case in the beam. Interference can exist between two channels ending up in the same final state, such as the "direct" channel (J) and the "diverted" one ($J-2$) leading to the same (J) state in the internal region (see Figure 1). The resulting interference terms vanish on averaging over an isotropic distribution of collisions (as in the bulk case). The present paper sets forth to analyze this interference effect and its consequences, using the approach of ref 1.

2. The Model

The collision of two atoms interacting with an electromagnetic field mode can be described by the Hamiltonian

$$\hat{H} = -\frac{1}{2\mu R^2}\frac{\partial}{\partial R}\left(R^2\frac{\partial}{\partial R}\right) + \frac{1}{2\mu R^2}(\hat{\mathbf{J}} - \hat{\mathbf{j}}_e)^2 + \hat{H}_e + \hat{H}_{rad} + \hat{V}_{rad} \quad (1)$$

using units in which $\hbar = 1$. Here, μ is the reduced mass of the colliding atoms, $\mathbf{R}$ is the radius vector of the relative motion,

* To whom correspondence should be addressed. E-mail: abram@post.tau.ac.il. Fax: +972-3-6409293.

10.1021/jp9819902 CCC: $15.00
Published on Web 11/03/1998

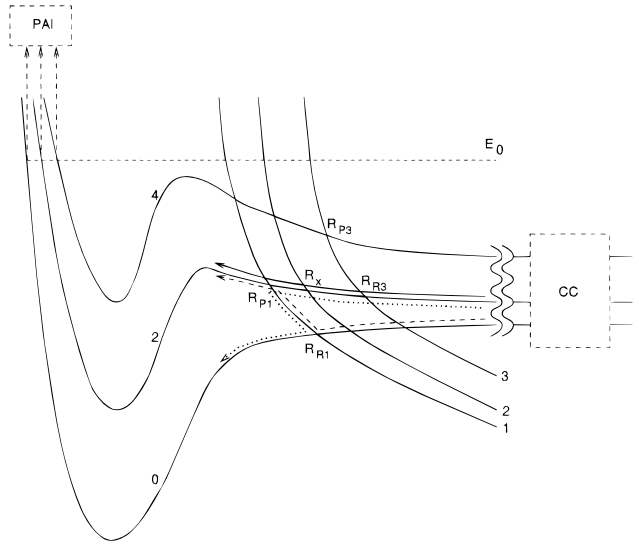

Figure 1. A schematic description of the potential curve arrangement. The numbers denote corresponding J values. The arrows describe the various penetration paths, discussed in the text (solid line for the direct, dashed line for the diverted, and dotted line for the counterintuitive). The PAI box represents the region of photoassociative ionization, and the CC box that of the coherent control.

$\hat{\mathbf{J}}$ is the total angular momentum operator (including the angular momentum of relative atomic motion and the resultant internal angular momentum $\hat{\mathbf{j}}_e$), $\hat{H}_e$ is the electronic Hamiltonian at fixed nuclear positions, $\hat{H}_{rad}$ is the Hamiltonian of the electromagnetic field with the eigenstates $|N\rangle_r$

$$\hat{H}_{rad}|N\rangle_r = N\omega|N\rangle_r \tag{2}$$

and $\hat{V}_{rad}$ is the interaction of the electrons with the electromagnetic field, defined here as

$${}_r\langle N|V_{rad}|N-1\rangle_r = -i\mathbf{E}\cdot\hat{\mathbf{d}}/2 \tag{3}$$

where $\mathbf{E}$ is the (linearly-polarized) electric field strength and $\hat{\mathbf{d}}$ is the total electronic dipole momentum operator.

The present work is concerned with the ${}^1\Sigma_g$ and ${}^1\Pi_u$ electronic states as representing, respectively, the ground and excited states of the diatom. In the adiabatic approximation, these states are eigenstates of $\hat{H}_e$ obeying

$$\hat{H}_e|\Lambda\rangle_e = V_{|\Lambda|}(R)|\Lambda\rangle_e, \quad \Lambda = 0, \pm 1 \tag{4}$$

where Λ is the projection of the electronic orbital angular momentum of the diatom on the molecular axes. The potential V_0 of the ${}^1\Sigma_g$ state is attractive and rather flat and V_1 of ${}^1\Pi_u$ state is repulsive. For our purpose, it suffices to use for V_0 the van der Waals interaction, and for V_1 the repulsive dipole−dipole interaction,

$$V_0(R) = -C_6/R^6, \quad V_1(R) = -\Delta + C_3/R^3 \tag{5}$$

Here Δ is the (blue-shifted) shielding-laser detuning, and (given d_r is the radial atomic dipole element) $C_3 = d_r^2/3$.

In the present paper, as in ref 1, we neglect the hyperfine structure effects and consider spinless ion cores leaving all internal angular momentum contributions to the outer-shell electrons. Thus, the full optical collision wave function must be symmetrical under exchange of the ion cores. It may be expanded in terms of the following basis functions, introduced in ref 13, combining the radiative, electronic, and rotational degrees of freedom

$$[|JM\Sigma\rangle = Y_{JM}(\vartheta,\varphi)|0\rangle_e|N\rangle_r \qquad (J \text{ even}) \tag{6}$$

$$|JM\Pi\rangle = i^J\left[\frac{2J+1}{8\pi}\right]^{1/2}[D^J_{1M}(\varphi,\vartheta,0)|\Lambda=+1\rangle_e + (-1)^J D^J_{-1M}(\varphi,\vartheta,0)|\Lambda=-1\rangle_e]|N-1\rangle_r \tag{7}$$

Here $D^J_{\Lambda M}(\varphi,\vartheta,0)$ are the Wigner functions (see ref 14), where ϑ and φ are the angular coordinates of $\mathbf{R}$ in relation to $\mathbf{E}$ (considered as a fixed quantization axis).

The close-coupling expansion of the system wave function in terms of the basis functions, eqs 6 and 7, has the form

$$\Psi = \sum_{J=0}^{\infty}{}' \sum_{M=-J}^{J} \frac{1}{R}\Phi^{(M)}_{J\Sigma}(R)|JM\Sigma\rangle + \sum_{J=1}^{\infty}\sum_{M=-J}^{J}\frac{1}{R}\Phi^{(M)}_{J\Pi}(R)|JM\Pi\rangle \tag{8}$$

where Σ' denotes a summation over only even values of J.

In order to consider the ionization processes in the internal region, we need as an asymptote the wave function $\Psi = \Psi_{in}$ including only incoming waves in its radial part. The plane-wave asymptotic stationary collision state forms a superposition $\Psi_{in} + \Psi_{out}$ at $R \to \infty$, where Ψ_{out} consists of outgoing radial waves, and can be written as

$$\Psi_{in} + \Psi_{out} \sim [\mu/2p_0]^{1/2}[\exp(i\mathbf{p}_0\mathbf{R}) + \exp(-i\mathbf{p}_0\mathbf{R})] \times |0\rangle_e|N\rangle_r + \text{scattered waves} \tag{9}$$

This state describes a unit incoming flux of particles with momentum $\boldsymbol{p}_0$, and has the proper symmetry with respect to ion-core exchange.[1] It then follows that the asymptotic conditions for the radial functions $\Phi^{(M)}_{J\Sigma}$ and $\Phi^{(M)}{}_{J\Pi}$ at $R \to \infty$ should be

$$\Phi^{(M)}_{J\Sigma} \sim A_{JM}(\mathbf{p}_0)\,[\mu/p_0]^{1/2}\exp(-ip_0R), \quad \Phi^{(M)}_{J\Pi} \sim 0 \tag{10}$$

where

$$A_{JM}(\mathbf{p}_0) = 2i\sqrt{2}\pi\frac{(-1)^J}{p_0}\,Y^*_{JM}\left(\frac{\mathbf{p}_0}{p_0}\right) \tag{11}$$

Transitions between the states of eqs 6 and 7 are governed by the matrix elements of the radiative coupling,

$$\langle J_0M_0\Sigma|V_{rad}|JM\Pi\rangle = (g^{(M)}_{RJ}\,\delta_{J-1,J_0} + g^{(M)}_{PJ}\,\delta_{J+1,J_0} + g^{(M)}_{QJ}\,\delta_{J,J_0})\delta_{MM_0} \tag{12}$$

where the three terms correspond to the three branches (R, P, and Q) of the optical rotational transition, and the coupling constants g are given in ref 1.

Substituting eq 8 into the stationary Schrödinger equation with Hamiltonian eq 1 (see ref 13), we obtain coupled equations for $\Phi^{(M)}_{J\Sigma}$ and $\Phi^{(M)}_{J\Pi}$.

As a consequence of these equations, each ground-level state $|JM\Sigma\rangle$ is coupled to the three excited states $|JM\Pi\rangle$, $|J\pm1M\Pi\rangle$ (except for $|JJ\Sigma\rangle$ that is coupled only to $|JJ\Pi\rangle$ and $|J+1J\Pi\rangle$, and $|00\Sigma\rangle$ that is coupled only to $|10\Pi\rangle$). The potential curves (including the centrifugal energy) of the states coupled with strengths $g^{(M)}_{RJ}$, $g^{(M)}_{PJ}$, and $g^{(M)}_{QJ}$ are crossing at the points R_{RJ}, R_{PJ}, and R_x, respectively (as in ref 1). Let us assume that the transition at each of the crossing points may be treated separately

using the LZ theory (see ref 16). This assumption does not allow us to take into account the counterintuitive transitions. The internal region can then be reached in the ground electronic state, with a given angular momentum J, along two possible paths: the direct one, including avoided crossings at the points R_{PJ-1}, R_x, and R_{RJ+1}, and the diverted one, including crossings at the points R_{RJ-1} and R_{PJ-1} (see Figure 1). An exception is the $J = 0$ state, which can be approached only by a direct path. Thus, the expression for the radial wave function $\Phi_{J\Sigma}^{(M)}(R)$ in the internal region consists of two terms, related to the corresponding penetration paths

$$\Phi_{J\Sigma}^{(M)} = (A_{JM}\sqrt{T_{JM}^{d}} - A_{J-2M}\sqrt{T_{JM}^{u}}\exp(i\chi_J^{(M)}))\xi_{J\Sigma} \quad (13)$$

Here, the penetration probabilities along the direct and diverted paths are respectively[1]

$$T_{JM}^{d} = \exp(-2\pi\lambda_{RJ+1}^{(M)} - 2\pi\lambda_{QJ}^{(M)} - 2\pi\lambda_{PJ-1}^{(M)}) \quad (14)$$

$$T_{JM}^{u} = [1 - \exp(-2\pi\lambda_{RJ-1}^{(M)})]\,[1 - \exp(-2\pi\lambda_{PJ-1}^{(M)})] \quad (15)$$

and $\xi_{J\Sigma}$ is a unit-flux normalized wave describing motion with angular momentum J in the field of the potential V_0 and the associated centrifugal potential. According to ref 1, the LZ exponents are given by

$$\lambda_{RJ}^{(M)} = \lambda_0\frac{(J+1)\,(J^2-M^2)}{J(2J-1)(2J+1)}\left[1 - \frac{(J-1)\,J}{J_x^{\,2}}\right]^{-1/2}\theta\,(J - |M|)$$

$$\lambda_{PJ}^{(M)} = \lambda_0\frac{J\,[(J+1)^2 - M^2]}{(J+1)(2J+1)(2J+3)}\left[1 - \frac{(J+1)(J+2)}{J_x^{\,2}}\right]^{-1/2} \times \theta(J+1 - |M|) \quad (16)$$

$$\lambda_{QJ}^{(M)} = \lambda_0\frac{M^2}{J(J+1)}\left[1 - \frac{J(J+1)}{J_x^{\,2}}\right]^{-1/2}\theta(J+1-|M|)$$

where, $\theta(x)$ is the Heavyside step function. Given the dipole−dipole interaction of eq 5

$$\lambda_0 \approx 3.31\times 10^2 (d_r\,(\mathrm{au}))^2 C_3^{\,1/3}(\mathrm{au})\Delta^{-4/3}(\mathrm{MHz})\left[\frac{\mu(\mathrm{amu})}{E_0(\mu\mathrm{K})}\right]^{1/2} \times I(\mathrm{W/cm^2}) \quad (17)$$

Here $E_0 = p_0^{\,2}/(2\mu)$, and I is the shielding-laser intensity, while

$$J_x^{\,2} = 2\mu E_0 (C_3/\Delta)^{2/3} \approx 4.04\times 10^{-2}\mu(\mathrm{amu})\,E_0(\mu\mathrm{K}) \times (C_3(\mathrm{au})/\Delta(\mathrm{MHz}))^{2/3} \quad (18)$$

As can be seen from eq 13, the amplitudes representing the direct and diverted paths may have different phases. The phase shift difference $\chi_J^{(M)}$ between these amplitudes is expressed in the semiclassical theory[16]) in the following form:

$$\chi_J^{(M)} = \chi\,(\lambda_{RJ-1}^{(M)}) - \chi\,(\lambda_{PJ-1}^{(M)}) + \int_{R_x}^{\infty}\{[2\mu(E_0 - V_{J-2}^{\mathrm{ad}}(R))]^{1/2} - [2\mu(E_0 - V_J^{\mathrm{ad}}(R))]^{1/2}\}\,\mathrm{d}R \quad (19)$$

consisting of a sum of contributions of the crossing points

$$\chi(\lambda) = \arg\Gamma(i\lambda) - \lambda\ln\lambda + \lambda + \pi/4 \quad (20)$$

and the difference between the phases produced by the adiabatic collision potentials V_{J-2}^{ad} and V_J^{ad}. The latter potentials are obtained by diagonalizing the potential matrix, including the diabatic potentials V_0 and V_1, the centrifugal potentials, and the radiative coupling V_{rad}. The subscript J corresponds here to the entrance-channel partial wave.

The efficiency of optical shielding is best measured by using one of the the ionization processes (photoionization in the case of alkali metal atoms, or Penning and associative ionization in the case of metastable rare-gas atoms), assuming that they occur at a closer range of the atomic separation. In order for the ionization process to occur, this close range must be first reached, by (a) crossing the shielding zone, and (b) passing over the centrifugal potential barrier (at $J > 0$ states). Let us assume for simplicity's sake that the three processes occur independently and that the crossing of the barrier merely implies $E_0 \geq V_b\,(J)$, where $V_b\,(J)$ is the height of the centrifugal barrier. We shall also further assume that, once the atoms entered the ionization region, past the centrifugal barrier, they will be ionized with a fixed probability, notwithstanding the partial wave J with which they have reached there. In this case, we can use the approach of ref 1 (see eq 4.4 therein) to write down the differential ionization cross section as

$$\sigma\,(\mathbf{p}_0) = \sum_{p_f}|\langle a,p_f|_r\langle N|S|\Psi(\mathbf{p}_0)\rangle|^2 \quad (21)$$

where $|a, p_f\rangle$ is a set of ion states. This set consists of outgoing waves with a proper normalization. The expression of eq 21 differs from the total cross section (see eq 4.1 in ref 1) by the absence of integration over the directions of the initial relative momentum $\mathbf{p}_0$ of the colliding atoms.

Using eqs 8, 11, and 13 for the wave function $\Psi(\mathbf{p}_0)$ one gets, up to a constant factor Z representing the fixed ionization probability

$$\sigma\,(\mathbf{p}_0) = \frac{8\pi^2}{p_0^{\,2}}\sum_{J=0}^{J_{\max}}{}'\sum_{M=-J}^{J}|\sqrt{T_{JM}^{d}}Y_{JM}\left(\frac{\mathbf{p}_0}{p_0}\right) - \sqrt{T_{JM}^{u}}Y_{J-2M}\left(\frac{\mathbf{p}_0}{p_0}\right)\exp(i\chi_J^{(M)})|^2 \quad (22)$$

where $J_{\max}$ is the maximal even number such that $V_b(J_{\max}) \leq E_0$. For the van der Waals potential of eq 5

$$J_{\max} = 2\left[\frac{1}{4}\left(\{1 + 12\mu\,(2E_0^{\,2}C_6)^{1/3}\}^{1/2} - 1\right)\right]$$

$$\approx 2\left[\frac{1}{4}\left(\{1 + 5.95\times 10^{-4}\mu\,(\mathrm{amu}) \times (E_0^{\,2}(\mu\mathrm{K})C_6(\mathrm{au}))^{1/3}\}^{1/2} - 1\right)\right] \quad (23)$$

where $[x]$ denotes the integer part of x.

Whenever it is necessary to drop the assumption of a fixed ionization probability, one can modify eq 22 by introducing within the summation signs a factor $Z_J^{(M)}$ representing a state-selective ionization probability starting from the partial wave of given J and M in the internal region.

In order to highlight explicitly the dependence on the angle ϑ between $\boldsymbol{p}_0$ and the electric field strength $\mathbf{E}$, let us express

the spherical harmonics in terms of the Legendre functions $P_J^{(M)}$ (see ref 15) and write the penetration probability as

$$P(\vartheta) = \frac{2}{(J_{\max}+1)(J_{\max}+2)} \times \sum_{J=0}^{J_{\max}}{}' \sum_{M=-J}^{J} [\tilde{T}^d_{JM} (P_J^{(M)}(\cos\vartheta))^2 + \tilde{T}^u_{JM} (P_{J-2}^{(M)}(\cos\vartheta))^2 + 2[\tilde{T}^d_{JM}\tilde{T}^u_{JM}]^{1/2} P_J^{(M)}(\cos\vartheta)\, P_{J-2}^{(M)}(\cos\vartheta) \cos\chi_J^{(M)}] \quad (24)$$

where

$$\tilde{T}^d_{JM} = (2J+1)\frac{(J-|M|)!}{(J+|M|)!} T^d_{JM}$$

$$\tilde{T}^u_{JM} = (2J-3)\frac{(J-2-|M|)!}{(J-2+|M|)!} T^u_{JM} \quad (25)$$

The three terms within the square brackets in eq 24 correspond, respectively, to the penetration along the direct path, the diverted path (see Figure 1), and the interference of these paths. The interference terms vanish on integration over directions of approach ($\mathbf{p}_0$). They are, therefore, absent in the penetration probability for an isotropic distribution of atomic velocities, as in the case of atomic traps, considered in ref 1. However, the interference must be taken into account in analyzing atomic-beam experiments.[12]

At low shielding-laser intensity we have $\tilde{T}^d_{JM} \gg \tilde{T}^u_{JM}$ and the interference term is negligible in comparison to the first term in the square brackets in eq 24 corresponding to the direct penetration path. The interference vanishes in the limit of high intensity, as well, i.e., when $\tilde{T}^d_{JM} \ll \tilde{T}^U_{JM}$. In this limit

$$P(\vartheta) \approx P_\infty = 1 - 2\frac{2J_{\max}+1}{(J_{\max}+1)(J_{\max}+2)} \quad (26)$$

does not depend on ϑ. The angle-averaged penetration probability, considered in ref 1, has the same "hangup" value P_∞. For the conditions prevailing in the Na beam experiment,[12] $J_{\max} = 4$ and $P_\infty = 0.4$. For the Xe bulk experiment,[3] considered in ref 1, $J_{\max} = 2$ and $P_\infty = 1/6$.

The interference terms substantially depend on the phaseshifts $\chi_J^{(M)}$. Unfortunately, their evaluation, in the adiabatic case, involves an infinite number of interacting channels. Because of this, and in order to show the full range of phaseshift variation, the penetration probabilities presented below include not only the phase shifts of eq 19, but also extremal values of the phase shifts.

Figure 2 presents the penetration probability as a function of the shielding-laser intensity, for several choices of cos $\chi_J^{(M)}$, calculated by using parameters appropriate to the Na beam experiment.[12] The results are compared with the experimental data of ref 12. This figure shows a strong influence of the interference on the penetration probability. The interference correction has the same sign as cos $\chi_J^{(M)}$ if the atomic beam and the electric field are parallel and the opposite sign if they are perpendicular. This effect follows from properties of the Legendre functions (see ref 15).

A better agreement with the experimental data may be obtained by choosing *M*-dependent phase shifts, such as cos $\chi_J^{(0)} = 0$ and cos $\chi_J^{(2)} = -1$ (see Figure 3). Phase shifts for other *M* values have no effect on these plots, since $P_J^{(M)}(0) = P_J^{(M)}(1) = 0$ for odd *M*.

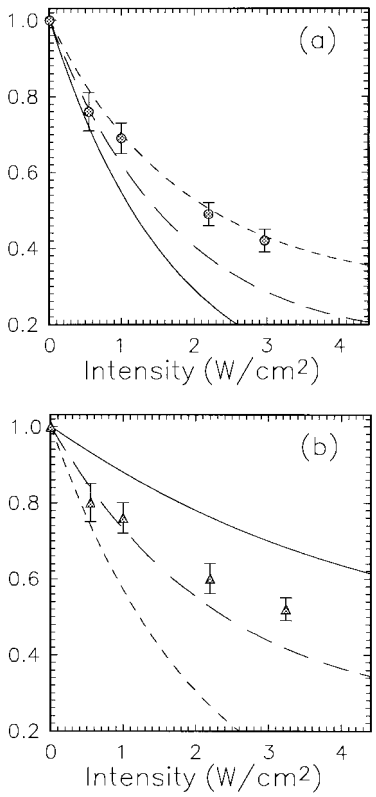

Figure 2. Penetration probability for Na as a function of the shielding-laser intensity at perpendicular (a) and parallel (b) polarization angles. Lines denote calculations using the semiclassical phase shifts (solid line), cos $\chi_J^{(M)} = 0$ (long-dashed line) or -1 (dashed line) for all *J* and *M*. The experimental data of Weiner and co-workers are shown for comparison, using the same laser detuning (250 MHz) and collision energy (60 mK) for all plots.

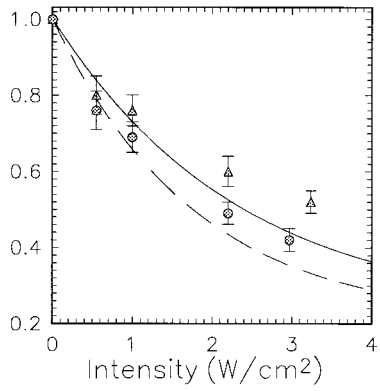

Figure 3. Penetration probability for Na as a function of the shielding-laser intensity is shown using a different set of phase shifts dependent on *M* [cos $\chi_J^{(0)} = 0$ and cos $\chi_J^{(2)} = 1$] but not on *J*. Calculated values for both polarizations [parallel (solid line) and perpendicular (dashed line)] are shown along with the experimental results. The results at these particular polarization angles are insensitive to $\chi_J^{(M)}$ with odd *M* values. Detuning and energy as in Figure 2.

The present model predicts non-monotonic dependence of the penetration probability on the shielding-laser intensity (see Figure 4), discernible on letting the laser intensity go beyond the maximum value used in the experiments.[12] The extent of this nonmonotonic variation, showing an optimization dip at a finite value of the laser intensity, is less pronounced in the bulk probabilities, as calculated for Xe in ref 1.

The angular dependence of the penetration probability at a fixed laser intensity is plotted in Figure 5. Only the plot for cos $\chi_J^{(M)} = 0$ (see Figure 5a) has a simple elliptical shape.

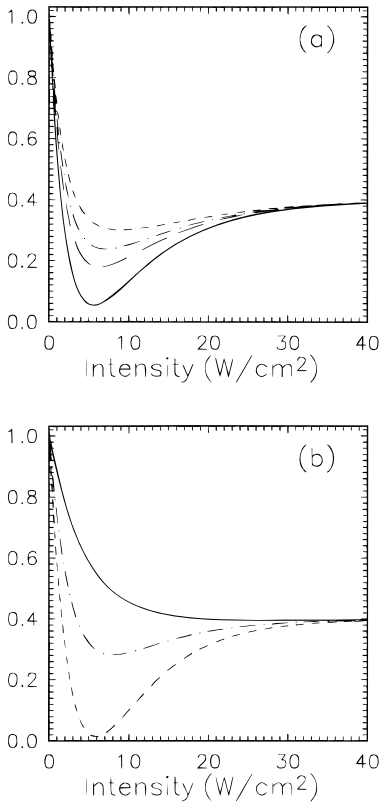

Figure 4. Penetration probability for Na calculated as a function of the shielding-laser intensity, at perpendicular (a) and parallel (b) polarization angles, plotted over an extended intensity range, to show the optimization dip at ≈6 W/cm^2. The phase shifts are as in Figure 2 (solid and dotted lines) or Figure 3 (dash-dotted line).

Unlike the cases of $\vartheta = 0$ and $\vartheta = \pi/2$ mentioned above, phase shifts $\chi_J^{(M)}$ having odd M values do affect the penetration probability at intermediate ϑ values.

3. Discussion

The present paper demonstrates the possibility of a substantial effect of interference on the optical shielding of beam atom collisions. This effect depends on the particular values of the relative phase shifts of the interfering channels. The semiclassical estimates based on eq 19 usually produce phase shift differences smaller than one radian, and therefore a significant interference effect (corresponding to cos $\chi_J^{(M)} \approx 1$). There is, however, no reason to rely exclusively on internal phase shifts, determined by the collision Hamiltonian only. A fleeting look at Figure 4 shows that, given a certain combination of the polarization angle and the phase shift, an almost complete shielding can be attained at a reasonably low laser intensity (∼6 W/cm^2), where the dip in the intensity-dependence curves may approach complete shielding. It would be therefore desirable to use the techniques of *coherent control* (refs 17 and 18) in order to obtain control over the phase shift difference. Whereas coherent control is usually applied to the *products* of certain processes, it should be applied here to the *reactants*, in the process of approaching the transition range. A possible application is a coherent stimulated-Raman device (with no resonance delay) with frequencies adjusted to a single Condon point, displaced sufficiently further out from the shielding zone.

Of course this would be optimally achieved if only one internal J state would matter, as each J state might require a different control scheme. It may nevertheless be possible to optimize the shielding by using a single control setup (at the cost of giving up almost complete shielding).

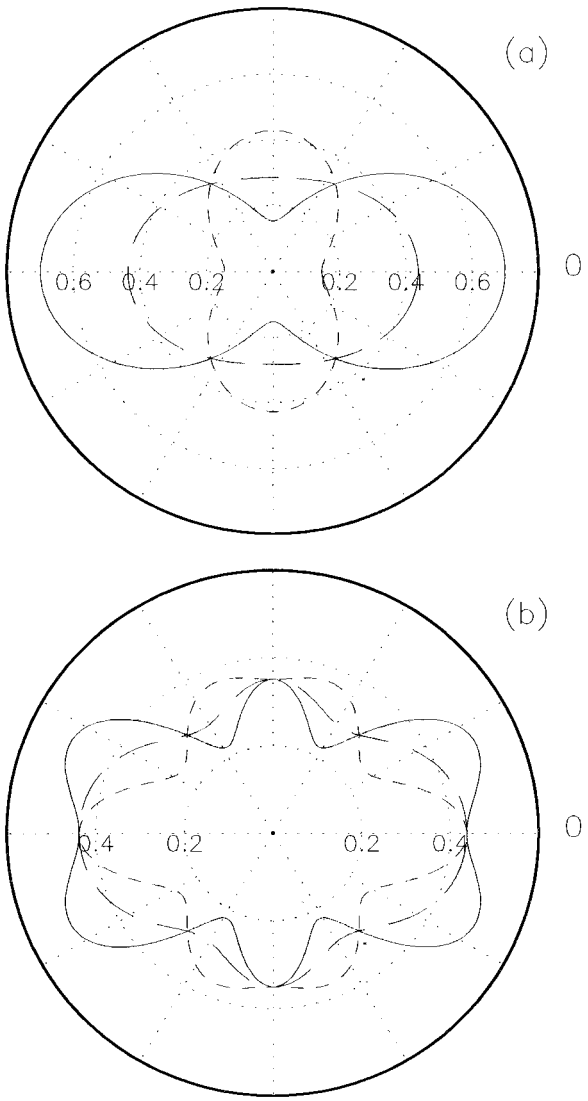

Figure 5. Penetration probability as a function of the polarization angle ϑ, for Na, calculated with a fixed laser intensity of $I = 3$ W/cm^2. Part a shows the three choices of phase shifts as in Figure 2. Part b shows the choice of phase shifts as in Figure 3, including several choices of $\chi_J^{(M)}$ [1 (solid line), 0 (long-dashed line), or −1 (dashed line)] for all odd M and all J values.

4. Conclusions

We have demonstrated here how channel interference can affect the optical shielding in the case of beams interacting in the presence of polarized radiation. In particular, we have pointed out the nonmonotonic dependence of the shielding efficiency on the laser intensity, and especially the way it depends on the polarization angle and on the phaseshift difference between the two interfering channels. Finally, we hinted at the possibility of coherently controlling this phase shift, exploiting the dip in the intensity dependence in order to optimize the shielding at a reasonably low value of the laser intensity.

Further experimental investigations, reaching slightly higher laser intensities than those used previously, will help clarify and establish the points considered here.

Acknowledgment. The authors are very grateful to John Weiner for prepublication results, and to him as well as to Paul Julienne and Moshe Shapiro for helpful discussions.

References and Notes

(1) Yurovsky, V. A.; Ben-Reuven, A. *Phys. Rev. A* **1997**, *55*, 3772.
(2) Napolitano, R.; Weiner, J.; Julienne, P. S. *Phys. Rev. A* **1997**, *55*, 1191.
(3) Suominen, K.-A.; Burnett, K.; Julienne, P. S.; Walhout, M.; Sterr, U.; Orzel, C.; Hoogerland, M.; Rolston, S. L. *Phys. Rev. A* **1996**, *53*, 1678. Walhout, M.; Sterr, U.; Orzel, C.; Hoogerland, M.; Rolston, S. L. *Phys. Rev. Lett.* **1995**, *74*, 506.
(4) Suominen K.-A.; Holland, M. J.; Burnett, K.; Julienne, P. S. *Phys. Rev. A* **1995**, *51*, 1446.
(5) Zilio, S. C.; Marcassa, L.; Muniz, S.; Horowicz, R.; Bagnato, V.; Napolitano, R.; Weiner, J.; Julienne, P. S. *Phys. Rev. Lett.* **1996**, *76*, 2033. Marcassa, L.; Horowicz, R.; Zilio, S. C.; Bagnato, V.; Weiner, J. *Phys. Rev. A* **1995**, *52*, R913. Marcassa, L.; Muniz, S.; de Queiroz, E.; Zilio, S. C.; Bagnato, V.; Weiner, J.; Julienne, P. S.; Suominen, K.-A. *Phys. Rev. Lett.* **1994**, *73*, 1911.
(6) Baly, S.; Hoffmann, D.; Walker, T. *Europhys. Lett.* **1994**, *27*, 273.
(7) Katori, H.; Shimizu, F. *Phys. Rev. Lett.* **1994**, *73*, 2555.
(8) Weiner, J. *Adv. At. Mol. Opt. Phys.* **1995**, *35*, 45.
(9) Suominen, K.-A. *J. Phys. B* **1996**, *29*, 5981.
(10) Yurovsky, V. A.; Ben-Reuven, A. *J. Phys. B* **1998**, *31*, 1.
(11) Yurovsky, V. A.; Ben-Reuven, A.; Band, Y.; Julienne, P. S., unpublished results.
(12) Tsao, C.-C.; Wang, Y.; Napolitano, R.; Weiner, J. *Eur. Phys. J. D*, in press.
(13) Julienne, P. S. *Phys. Rev. A* **1982**, *26*, 3299.
(14) Landau, L. D.; Lifshitz, E. M. *Quantum Mechanics*; Pergamon: Oxford, UK, 1977.
(15) *Handbook of Mathematical Functions*; Abramovitz, M., Stegun, I. E., NBS: Washington, DC, 1964.
(16) Child, M. S. *Semiclassical Mechanics with Molecular Applications*; Clarendon Press: Oxford, UK, 1991.
(17) Shapiro, M.; Brumer, P. *J. Chem. Soc., Faraday Trans.* **1997**, *93*, 1263.
(18) Gordon, R. J.; Rice, S. A. *Annu. Rev. Phys. Chem.* **1997**, *48*, 601.